



MEASURING GESTATIONAL AGE AND UTERINE DIAMETER BASED ON IMAGE SEGMENTATION

Retno Supriyanti¹, Ahmad Abdul Hafidh¹, Yogi Ramadhani¹ and Haris B Widodo²

¹Electrical Engineering Department, Jenderal Soedirman University, Indonesia

²Medical Faculty, Jenderal Soedirman University, Indonesia

E-Mail: retno_supriyanti@unsoed.ac.id

ABSTRACT

This paper will discuss the application of image processing techniques in the medical field, especially in the calculation of the age of the fetus and uterine diameter at ultrasonography with low-resolution image. We applied image morphology and edge detection method in the segmentation process. The main objective of this research is to confirm the diagnosis of a gynaecologist or health workers who are in the rural areas where health facilities are limited so that the image of the existing ultrasonography has a low quality or just a print out of ultrasonography in other areas. So that further analysis is required on that image. Experimental results show that the system that we have developed has a maximum error 5.3%. Therefore it can be said that this system has a performance that promises to be developed further.

Keywords: gestational age, uterine diameter, image segmentation, morphological image, edge detection.

1. INTRODUCTION

Information technology is developing very rapidly at this time. One field of information technology is experiencing rapid development is digital image processing techniques. These techniques are widely applied in various fields one of which is the medical field.

As we all know, one form of technology which is applied in the medical field is the use of ultrasonography machine. One use of the ultrasonography machine is in the field of obstetrics and gynaecology. In general, the first ultrasonography performed at 7 weeks gestation to ensure state of pregnancy. In the ultrasonography examination will assess the fetal heart rate, measuring the length of the fetus to assess gestational age. Second ultrasonography examination is usually done at 18-22 weeks gestation to assess congenital abnormalities, deformities, placental position, fetal heart rate, as well as to assess the development of the fetus. In the third ultrasonography examination is usually performed at 34 weeks' gestation for evaluate the size of the fetus and fetal growth rate, movement and breathing, the baby's heartbeat and the amount of amniotic fluid surrounding the baby as well as the position of the baby and placenta. Basically, ultrasonography can be done anytime during pregnancy, because ultrasonography is not dangerous for mother and baby. Ultrasonography examinations are mainly carried out when there is a problem pregnancy[1]. Referring to the usefulness of the ultrasonography machine, it is seen that the use of this machine is quite important in the diagnosis. In other hand, digital image processing is one of information technology field. Image Processing is a technique to improve the original image received from the camera for a variety of applications. This field of image processing significantly increased the current and widely applied in various fields; including the medical field in particular is a medical imaging.

Some research that discusses medical imaging in particular ultrasonography image are as follows. Supriyanti [2] discussed the use of template matching to localize the part of the uterus that will be explored further

automatically from the low-quality ultrasonography images. Kwok [3] in his research used harmonic method to describe the prostate boundary. Harmonic method using Fourier information to remove noise and encodes a thin boundary. Lam [4] He proposed a series of image processing methods including image enhancement, image segmentation and edge detection before measuring appendix. Selection of image enhancement method which is based on the MSE and PSNR in the image is segmented and time required. Flores [5] he proposed an adaptive contrast enhancement method based sigmoidal mapping function is used to segment the image of ultrasonography in breast tissue. Potocnik [6] conducted a survey of a wide variety of image processing methods exist for the detection, recognition, and analysis of the follicle in two-dimensional (2-D) and 3-D footage ovarian ultrasound. Their study focused on efficiency, validation, and assessment of follicular processing algorithms. Luo [7] tried to validate the accuracy of the patient's coronary artery lumen region obtained from CT images based on intravascular ultrasound (IVUS). Salmon [8] presented an overview of clinical intraoral ultrasonography that can be completely interpreted, to identify relevant applications. Wang [9] developed diffusion filters that apply local deviation standards and edge detection to determine adaptive end termination functions in diffusion filtering. It is used to overcome the lack of traditional diffusion filters. Kim [10] developed diffusion filters that apply local deviation standards and edge detection to determine adaptive end termination functions in diffusion filtering. It is used to overcome the lack of traditional diffusion filters. Evans [11] described the various components of the basic CFI system needed to produce speed information and combine it with anatomical information. He then describes a number of variations on basic autocorrelation techniques, including cross-correlation based techniques, power Doppler, Doppler network imaging, and 3D Doppler imaging (3D). Zhang [12] developed a computerized system that distinguishes cervical lymph nodes on ultrasonography because of malignant or benign.



He used ten quantitative features that represent sonography features of size, margin, nodal border, shape, medulla ratio, medulla distribution, echogenicity, echogeneity, vascular density, and vascular patterns, each calculated based on node contours segmented by more snake models good. Deng [13] developed a prototype device that allows the examination of orofacial anatomy 3D and 4D. He made improvements to the device and increased 4D acquisition time by proposing new methods of dynamic imaging and counting many soft-tissue components in 3D. Kim [14] In his research, he made measurements about Hepatorenal index differences between the liver and kidney based on the severity of the disease. He uses a series of image processing techniques such as the use of stretching techniques and blurred edges, applied to extract the inters region. Mahmoud [15] In his research, he conducted an experiment to test the feasibility of using high-frequency ultrasonography imaging systems specially designed to reconstruct three-dimensional (3D) surface images of periodontal damage to human jawbone. According to the research above, most of research subject used complex methods to apply in medical images. The aim of this research is to improve image quality especially uterus region produced by low-resolution ultrasonography. The goal is based on the fact that there are in developing countries like Indonesia, where for many areas, existing medical equipment especially ultrasonography machine is low resolution quality. However in this paper, we emphasize on measuring gestational and utrine diameter automatically based on image segmentation.

In our previous research [16] [17] [18] [19] [20] [21] [22] [23] [24] [25] [26] [27] [28] [29] [30] [31] [32] [33] [34] [35] [36] [37] We are focusing on digital image processing applications on quality improvement and medical image function. In this paper we emphasize on improving the automatic function of image processing application in determining the diameter and estimate of gestational age in low quality ultrasound image.

2. RESEARCH METHODS

The field of obstetrics and gynaecology on medical uses ultrasonography devices to estimate gestational age, estimate delivery day and to visualize maternal fetal development. This is because it is easy to use, and this examination is minimally invasive to mother and fetus. However this ultrasonography examination requires special skills from its users, because the accuracy of this ultrasound results depends on the user's skill. In addition, the resulting image quality factor also affects the diagnosis.

Currently existing ultrasonography machines have three-dimensional or four-dimensional. However, for developing countries like Indonesia, the availability of such machines is still limited in big cities only. In addition the equipment is quite expensive so the patient must pay more expensive as well. For that reason, in many regions of Indonesia still use 2 dimensional ultrasonography machine. As a note, the ultrasonography machines in the rural area have a low resolution and some required functions must be run manually. Also, in some areas, there

is no ultrasonography available at all. As described in the previous sub section, in this paper we will discuss about the use of image processing techniques in estimating gestational age and uterine diameter.

2.1. Determining gestational age

Gestational age is different from fetal age. Fetal age is based on the normal ovulation cycle of about 14 days after menstruation. If a woman has a 28 day and regular menstrual cycle, usually the fetus age has a 2 week gestational age. In other words, when a woman is 8 weeks pregnant, then the age of the fetus is 6 weeks. Meanwhile, the determination of gestational age based on ultrasonography examination could be done in 2 ways [38]: (i) Measuring the diameter of fetal sac (Mean Sac Diameter) is described in Equation 1.

$$MSD = \frac{p + l + t}{3} \quad (\text{Eq. 1})$$

Wherein:

p = length (mm)

l = width (mm)

t = height (mm)

Estimated gestational age could use the formula as described in Equation 2:

$$\delta t = MSD + 30 \text{ days} \quad (\text{Eq. 2})$$

Wherein:

δt = Gestational age (days)

MSD = mean sac diameter (1day/1mm after 30 days)

Figure-1 described an example of fetus sac diameter.



Figure-1. An example of fetal sac diameter.

(ii) Measuring distance between head-butt fetal (Crown Rump Length/CRL)

We can estimate gestational age using formula as described in Equation 3.

$$\delta t = CRL + 6.5 \text{ weeks} \quad (\text{Eq. 3})$$

Wherein:

δt = Gestational age (weeks)

CRL = Crown Rump Length (mm)

2.2. Data acquisition

As already explained in the paragraph above, that the input data is a digital image scanning the uterine



region by using a low-resolution ultrasonography machine. If the image data received in the form of print out, then the image is scanned by using a scanner machine manually. Figure-2 is an example of the data input used in this research.



Figure-2. Examples of input data.

The input data is then fed into the system we developed using matlab. We developed the system using the matlab GUI as seen in Figure-3.

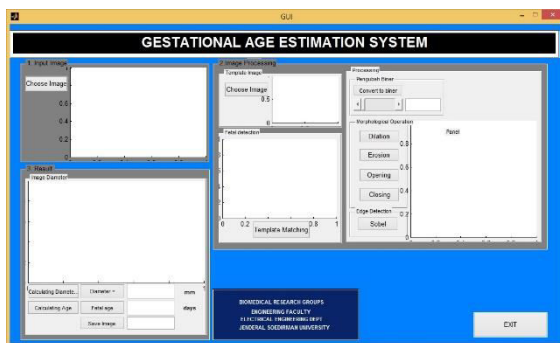


Figure-3. Display of our system.

The explanation of GUI as appear in Figure-3 can be explained as follows. The GUI has 15 push buttons, 5 axes, 1 slider, 4 text editing, 7 static texts, 7 panels. Push button is a button to perform an action or a call. Axes serves as a place to display images. Slider serves to set the input numbers for the threshold so that users can easily change the number of threshold that has a range of 0 - 1 by shifting the control on the slider. Edit text is a control that serves to insert and change text in the form of data strings. Static text is a control that serves to create text labels, and is static. Panel is a box that serves to group specific areas.

2.3. Image processing process

This panel is divided into 3 panels, namely Image Template panel, Fetal Detection panel, Image Processing Operation panel. Here's an explanation of each panel :(i) Image Template Panel has a function to call predefined templates. The template command is as follows:

```
[filenamepathname]= uigetfile({'*.jpg'; '*.bmp'}, 'Select an Image');
imgname=[pathname filename];
axes(handles.gambartemplate);
imshow(imgname);
```

Uigetfile to search the image file, then it will be saved in the form of filename and pathname matrix. Then this matrix will be displayed on axes via axes command

(handles.gambartemplate); Then the image will be displayed on the axes named *gambartemplate*. The matrix will be displayed on the image template via the *imshow* command (*imgname*). After the template call is complete, it can be continued with fetal detection. (ii) Fetal Detection Panel: The fetal image detection program has a function to crop the image to facilitate the search of fetal image diameter. This detection stage uses the template matching method, which is an image matching method by finding the smallest parts and matching the image template. Template image testing results will be presented in the Results and Discussions section. (iii) Image Processing Operation Panel: It is divided into 3 parts, namely: binary converter panel, morphology operation panel and edge detection panel. Here's an explanation from each panel: (a) Binary Converter: has a function to convert grayscale image into binary image. Source code of the binary change function:

```
c=getimage(handles.citra_hasil_deteksi);
d=im2bw(c);
axes(handles.operasimorfologi);
imshow(d);
```

The image generated from the "UbahBiner" button is then invoked for display using the *imshow* (*d*); function. The image that appears in "operasimorfologi" axes will be recalled to continue the adaptive thresholding process. This process is useful to obtain a clearer picture and get an optimal value because each image has different color intensity. The results of adaptive threshold experiments will be presented in the Results and Discussions section. (b) Morphology Operation Panel: Morphological operation is a step to clean up the image after the image is altered binary. There are several push buttons on the morphology operation i.e., push button dilation, erosion, opening and closing. (c) Edge detection: has a function to clarify the borders of the usg image. Use of edge detection is only done if the borders of the image are not clearly visible. However, if the peripheral borders are clearly visible then no edge detection is performed.

3. RESULTS AND DISCUSSIONS

As discussed in subsection 2, we use image template method. Figure-4 shows our image template for evaluating which is the best template image for the next process in our system.

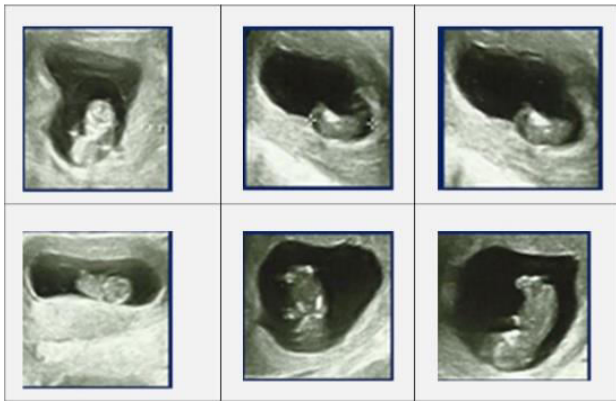


Figure-4. Image templates in our experiment.

After testing the template to find out which template can be used to detect all ultrasound images then obtained the results as shown in Figure-5.

No.	Original image	Image Detection Results					
		Template 1	Template 2	Template 3	Template 4	Template 5	Template 6
1							
2							
3							
4							
5							
6							

Figure-5. Image detection results.

Referring to Figure-5, we can calculate the performance of image template matching for each template as described in Table-1.

Table-1. Performance of image template matching.

Template	Performance
Template 1	100 %
Template 2	33.3%
Template 3	33.3%
Template 4	66.6%
Template 5	50%
Template 6	33.3%

The performance results of the six template images are then used to clean the image using morphological and edge detection operations.

Based on Table-1, template1 has the greatest performance that is 100%. Therefore Template 1 is used as an image template throughout this experiment.

The processing time of this matching template depends on the image resolution of the original image. Large resolution has a larger number of pixels so the resulting image is smoother. The template matching process is done on the grayscale image. In this process the original image will be changed first converted to grayscale image. The next step of the ultrasound image is the matching process with the template provided.

In the binary converting process, we use adaptive threshold. The threshold value is changed using a slider where the slider will change the threshold from 0 to 1. This threshold value change is performed by the user. Figure-6 shows an example of using adaptive threshold.

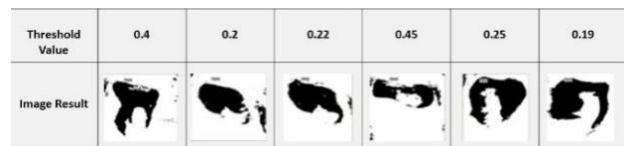


Figure-6. An example of adaptive threshold values.

Referring to Figure-6, it can be concluded that the appropriate adaptive threshold for the image is 0.45. Therefore, the image will use threshold 0.45. Once the threshold value is obtained correctly, then continued morphological and edge detection operations to get the best contour.

After the morphological operation, it will get the form of the fetus intact so that can be measured the fetal diameter. The longest distance of the image is assumed to be the average diameter of the image. Figure-7 shows examples of calculating fetal diameter.

Image Result						
Diameter (mm)	47	33	41	58	50	45

Figure-7. An example of image diameter values.

The pregnancy age in the image can be determined by entering the MSD formula (Equation 2) into the source code. By combining the MSD formula to the diameter source code as follows.

```
usia = MSD+30;
set(handles.hasilusia, 'string', usia);
axes(handles.axes6);
```

Source code formula age = MSD + 30; Where the MSD is taken from the diameter result. The sum of MSD with variable 30 means that gestational age is calculated from 30 days. The fetal sac will expand by 1mm / day. Table-2 shows some examples of pregnancy age based on diameter.

**Table-2.** Examples of pregnancy age based on diameter.

Diameter (mm)	Pregnancy age (days)
47	77
33	73
41	71
58	88
50	80
45	75

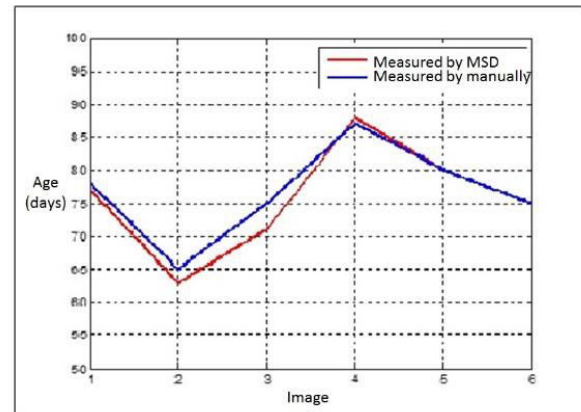
Some of the parameters that affect the results include: threshold value, number of morphological operations and edge detection, and also errors from gestational age.

According to the threshold, each image gets different threshold treatment. The threshold value determines the quality of the image to be processed further so that the accurate diameter and gestational age is obtained. The threshold value has a range between 0 and 1. In the GUI view, the threshold value can be set and selected between the ranges.

According to the morphological operations, Morphological and edge detection operations are performed on the image of the "change binary" after the thresholding stage. Each image differs in the way of treatment, depending on how the condition of the image after the threshold. In morphological operations, dilation and erosion and edge detection of the sobel can be enlarged, by pressing the puss button more than once or reduced. This is done to get a better image. Figure 8 shows an example of morphological operation in an image.

**Figure-8.** An example of morphological operation.

As a comparison, we also did the calculation of gestational age manually. The original USG image is manually measured using paint. The first step of inputting the original image to the paint is then measured by spreading a straight line. Straight line is seen based on the result of image calculation using Matlab. Once known coordinates of each point in units of pixels and then converted into units of mm. Where 1 pixel = 0.26458 mm. The diameter of the image is measured using the pythagoras formula. The value of gestational age generated by the formulation of MSD can be tested for success rate by comparing pregnancy age of MSD calculation result with manual calculation. Figure-9 shows comparison of gestational age calculated by MSD and manually.

**Figure-9.** Comparison graph of gestational age calculated by MSD and manually.

Some factors that have potential for generating an error are: (i) Original USG images obtained with low resolution and less obvious contrast. (ii) Resize the original image of ultrasound, so the ultrasound image has scale. (iii) Not all morphological operations are used. The operations used are only related to image cleanup.

The mean age of MSD calculation results for the entire image is 75.67 days and the data distribution for the age score of the MSD calculation result has a standard deviation of 8.43. The mean age of manual calculations for the overall image is 76.67 days and the data distribution for the age value of the manual calculation has a standard deviation of 7.23.

4. CONCLUSIONS

Based on the results of the research of edge detection and morphological operation, on medical USG image to determine gestational age with variable of uterine diameter, the conclusion is as follows: (i) the diameter value of MSD calculation results from images obtained between 33 mm to 58 mm. The diameter value of the manual calculation results from the image obtained between 35 mm to 57 mm (ii) Age of pregnancy MSD calculation results from images obtained between 63 days to 88 days. Gestational age of manual calculation results from images obtained between 65 days to 87 days. (iii) The threshold value of the image is 0.19 to 0.45.

The calculation result of gestational age has error value up to 5.3% with accuracy level equal to 94.7%. This system is promising to be applied to rural and child health centres in rural areas so they can get an accurate gynecological screening service.

ACKNOWLEDGEMENT

This work is supported by Directorate General of Education through "Penelitian Strategis Nasional (STRANAS)" fiscal academic year 2014-2015.

REFERENCES

- [1] S. K. Edelman. 2004. Understanding Ultrasound Physics. E.S.P. Ultrasound.



- [2] R. Supriyanti, I. A. Pradana, E. Murdyantoro and H. B. Widodo. 2014. Localizing Uterus Region from Low-Resolution Ultrasonography Device Using Template Matching Method. *Int. J. Biosci. Biochem. Bioinforma.* 4(5): 304-311.
- [3] C. K. Kwok, M. Y. Teo, W. S. Ng, S. N. Tan and L. M. Jones. 1998. Outlining the prostate boundary using the harmonics method. *Med. Biol. Eng. Comput.* 36(6): 768-771.
- [4] J. Lam, C. Pahl, H. N. Abduljabbar, and E. Supriyanto. 2014. Measurement and Analysis of the Diameter of Appendix Based on Ultrasound Images. *Int. J. Biosci. Biochem. Bioinforma.* 4(2): 130-136.
- [5] W. G. Flores and W. C. de A. Pereira. 2017. A contrast enhancement method for improving the segmentation of breast lesions on ultrasonography. *Comput. Biol. Med.* 80(no. May 2016): 14-23.
- [6] B. Potocnik, B. Cigale and D. Zazula. 2012. Computerized detection and recognition of follicles in ovarian ultrasound images: A review. *Med. Biol. Eng. Comput.* 50(12): 1201-1212.
- [7] T. Luo, T. Wischgoll, B. K. Koo, Y. Huo and G. S. Kassab. 2014. IVUS validation of patient coronary artery lumen area obtained from CT images. *PLoS One.* 9(1): 1-8.
- [8] B. Salmon and D. Le Denmat. 2012. Intraoral ultrasonography: Development of a specific high-frequency probe and clinical pilot study. *Clin. Oral Investig.* 16(2): 643-649.
- [9] S. R. Wang, Y. N. Sun, and F. M. Chang. 2016. Artifact removal and texture-based rendering for visualization of 3D fetal ultrasound images. *Med. Biol. Eng. Comput.* 46(6): 575-588.
- [10] K. B. Kim, D. H. Song and H. J. Park. 2016. Automatic Extraction of Appendix from Ultrasonography with Self-Organizing Map and Shape-Brightness Pattern Learning. *Biomed Res. Int.* 2016: 5206268.
- [11] D. H. Evans and P. N. T. Wells. 2010. Colour flow and motion imaging. *Proc. Inst. Mech. Eng. Part H J. Eng. Med.* 224(2): 241-253.
- [12] J. Zhang, Y. Wang, Y. Dong and Y. Wang. 2008. Computer-aided diagnosis of cervical lymph nodes on ultrasonography. *Comput. Biol. Med.* 38(2): 234-243.
- [13] J. Deng, M. Nina, A. Margaret and A. Rebecca. 2009. Novel technique for three-dimensional visualisation and. *Lancet.* 356: 127-131.
- [14] K. B. Kim and C. W. Kim. 2015. Quantification of Hepatorenal Index for Computer-Aided Fatty Liver Classification with Self-Organizing Map and Fuzzy Stretching from Ultrasonography. *Biomed Res. Int.* 2015: 1-9.
- [15] A. M. Mahmoud, P. Ngan, R. Crout and O. M. Mukdadi. 2010. High-resolution 3d ultrasound jawbone surface imaging for diagnosis of periodontal bony defects: An in vitro study. *Ann. Biomed. Eng.* 38(11): 3409-3422.
- [16] R. Supriyanti, H. Habe, M. Kidode and S. Nagata. 2009. Extracting Appearance Information inside the Pupil for Cataract Screening. in 11th IAPR Conference on Machine Vision Applications. pp. 342-345.
- [17] R. Supriyanti, E. Pranata, Y. Ramadhani and T. I. Rosanti. 2013. Separability Filter for Localizing Abnormal Pupil: Identification of Input Image. *Telkomnika.* 11(4): 783-790.
- [18] R. Supriyanti, H. Habe, M. Kidode and S. Nagata. 2008. A simple and robust method to screen cataracts using specular reflection appearance. in *Proc. SPIE 6915 Medical Imaging.*
- [19] R. Supriyanti, I. A. Pradana, E. Murdyantoro, and H. B. Widodo. 2014. Localizing Uterus Region from Low-Resolution Ultrasonography Device Using Template Matching Method. *Int. J. Biosci. Biochem. Bioinforma.* 4(5): 304-311.
- [20] R. Supriyanti, Y. Ramadhani, H. Habe, M. Kidode, and S. Nagata. 2010. Performance of Various Digital Cameras for Cataract Screening Techniques based on Digital Images. in *Proceeding of International Seminar of Electrical Power, Electronics, Communications, Control and Informatics (EECCIS).*
- [21] R. Supriyanti, H. Habe, M. Kidode and S. Nagata. 2009. Compact cataract screening system : Design and practical data acquisition. in *Proceeding of International Conference on Instrumentation, Communications, Information Technology, and Biomedical Engineering (ICICI-BME).* pp. 1-6.
- [22] R. Supriyanti, H. Habe, M. Kidode and S. Nagata. 2009. Cataract Screening by Specular Reflection and Texture Analysis. *J. Commun. SIWN.* 6(1): 59-64.



- [23] R. Supriyanti, A. Inomata and K. Fujikawa. 2012. Tele-Ophthalmology for Rural Areas in Indonesia: Preliminary Study of Image Acquisition Rate Using Various Bandwidths. 2012 Int. Conf. Environ. Sci. Engineering. 3: 165-170.
- [24] R. Supriyanti, M. Kidode, H. Habe, and S. Nagata. 2011. Low-Cost and Easy-to-Use Equipment for Cataract Screening based on Digital Images. in Proceeding of The 12th International Conference on Quality in Research (QIR).
- [25] R. Supriyanti and Y. Ramadhani. 2011. The Achievement of Various Shapes of Specular Reflections for Cataract Screening System Based on Digital Images. 2011 Int. Conf. Biomed. Eng. Technol. 11: 75-79.
- [26] R. Supriyanti, T. Budiono, Y. Ramadhani, H. B. Widodo, and A. Mulyawati. 2015. Pre-Processing of Ultrasonography Image Quality Improvement in Cases of Cervical Cancer Using Image Enhancement. Int. Conf. Biomed. Imaging. 2(8): 1318-1322.
- [27] R. Supriyanti, D. Putri, E. Murdyantoro and H. B. Widodo. 2013. Comparing edge detection methods to localize uterus area on ultrasound image. In International conference of Instrumentation, Communications, Information Technology, and Biomedical Engineering (ICICI-BME). pp. 152-155.
- [28] R. Supriyanti, A. W. D. Susilo, Y. Ramadhani, A. Mulyawati and H. B. Widodo. 2015. Extraction of Ultrasonography Images Using Ratio of Geometric Operations. J. Med. Bioeng. 4(3): 206-212.
- [29] R. Supriyanti, T. Septiana, Y. Ramadhani, E. Murdyantoro and H. B. Widodo. 2013. Analytical Hierarchy Process for Estimating Pregnancy Diseases. in Proceeding of International Conference on Conference on Biomedical Science and Engineering. pp. 1003-1007.
- [30] R. Supriyanti and Y. Ramadhani. 2012. Consideration of Iris Characteristic for Improving Cataract Screening Techniques Based on Digital Image. 2012 2nd Int. Conf. Biomed. Eng. Technol. 34: 126-129.
- [31] R. Supriyanti, B. Setiawan, H. B. Widodo, and E. Murdyantoro. 2012. Detecting Pupil and Iris under Uncontrolled Illumination using Fixed-Hough Circle Transform. Int. J. Signal Process. Image Process. Pattern Recognit. 5(4): 175-189.
- [32] R. Supriyanti, S. Suwitno, H. B. Widodo and T. I. Rosanti. 2016. Brightness and Contrast Modification in Ultrasonography Images Using Edge Detection Results. TELKOMNIKA (Telecommunication Comput. Electron. Control. 14(3): 1090-1098.
- [33] R. Supriyanti, A. S. Setiadi, Y. Ramadhani, and H. B. Widodo. 2016. Point Processing Method for Improving Dental Radiology Image Quality. Int. J. Electr. Computer Eng. 6(4): 1587-1594.
- [34] R. Supriyanti, U. Erfayanto, Y. Ramadhani, E. Murdyantoro and H. B. Widodo. 2016. Blood Pressure Mobile Monitoring for Pregnant Woman Based Android System. IOP Conf. Ser. Mater. Sci. Eng. Vol. 105.
- [35] H. B. Widodo, A. Soelaiman, Y. Ramadhani, and R. Supriyanti. 2015. Calculating Contrast Stretching Variables in Order to Improve Dental Radiology Image Quality. Int. Conf. Eng. Technol. Sustain. Dev. 12002(82).
- [36] R. Supriyanti, G. Satrio, Y. Ramadhani, and W. Siswandari. 2017. Contour Detection of Leukocyte Cell Nucleus Using Morphological Image. J. Phys. Conf. Ser. 824(1).
- [37] R. Supriyanti, A. Fariz, T. Septiana, E. Murdyantoro, Y. Ramadhani, and H. B. Widodo. 2015. A Simple Screening for High-Risk Pregnancies in Rural Areas Based Expert System. Telkomnika. 13(2): 661-669.
- [38] G. F. N. F. G. Cunningham, K. J. Leveno, L. C. Gilstrap, J. C. Hauth and K. D. Wenstrom. 2005. Williams Obstetrics 22nd edition. New York, USA: McGRAW -HILL.